

University of Groningen

Mechanisms controlling the air–sea CO₂ flux in the North Sea

Prowe, A.E.F.; Thomas, Helmut; Pätsch, Johannes; Kühn, Wilfried; Bozec, Yann; Schiettecatte, Laure-Sophie; Borges, Alberto V.; Baar, Hein J.W. de; Paetsch, J; Kuehn, W

Published in:
Continental Shelf Research

DOI:
[10.1016/j.csr.2009.06.003](https://doi.org/10.1016/j.csr.2009.06.003)

IMPORTANT NOTE: You are advised to consult the publisher's version (publisher's PDF) if you wish to cite from it. Please check the document version below.

Document Version
Publisher's PDF, also known as Version of record

Publication date:
2009

[Link to publication in University of Groningen/UMCG research database](#)

Citation for published version (APA):

Prowe, A. E. F., Thomas, H., Pätsch, J., Kühn, W., Bozec, Y., Schiettecatte, L-S., Borges, A. V., Baar, H. J. W. D., Paetsch, J., & Kuehn, W. (2009). Mechanisms controlling the air–sea CO₂ flux in the North Sea. *Continental Shelf Research*, 29(15), 1801-1808. <https://doi.org/10.1016/j.csr.2009.06.003>

Copyright

Other than for strictly personal use, it is not permitted to download or to forward/distribute the text or part of it without the consent of the author(s) and/or copyright holder(s), unless the work is under an open content license (like Creative Commons).

The publication may also be distributed here under the terms of Article 25fa of the Dutch Copyright Act, indicated by the “Taverne” license. More information can be found on the University of Groningen website: <https://www.rug.nl/library/open-access/self-archiving-pure/taverne-amendment>.

Take-down policy

If you believe that this document breaches copyright please contact us providing details, and we will remove access to the work immediately and investigate your claim.

Downloaded from the University of Groningen/UMCG research database (Pure): <http://www.rug.nl/research/portal>. For technical reasons the number of authors shown on this cover page is limited to 10 maximum.



Mechanisms controlling the air–sea CO₂ flux in the North Sea

A.E.F. Prowe^{a,b,c,*}, Helmuth Thomas^{a,c}, Johannes Pätsch^d, Wilfried Kühn^d, Yann Bozec^{c,e}, Laure-Sophie Schiettecatte^f, Alberto V. Borges^f, Hein J.W. de Baar^c

^a Department of Oceanography, Dalhousie University, 1355 Oxford Street, Halifax, NS, Canada B3H 4J1

^b IFM-GEOMAR, Leibniz Institute of Marine Sciences at the University of Kiel, Düsterbrookweg 20, 24105 Kiel, Germany

^c Royal Netherlands Institute for Sea Research (NIOZ), Landsdiep 4, 1797 SZ 't Horntje, The Netherlands

^d Institute of Oceanography, University of Hamburg, Bundesstr. 53, 20146 Hamburg, Germany

^e Station Biologique de Roscoff, CNRS et UPMC Univ. Paris 06, UMR 7144 - Chimie Marine, Place Georges Teissier, BP74, 29682 Roscoff, France

^f Chemical Oceanography Unit, University of Liège, Allée du 6 Août, 17, 4000 Liège, Belgium

ARTICLE INFO

Article history:

Received 26 February 2009

Received in revised form

19 May 2009

Accepted 17 June 2009

Available online 25 June 2009

Keywords:

CO₂ air–sea flux

Continental shelf pump

Biogeochemical modelling

ECOHAM

North Sea

ABSTRACT

The mechanisms driving the air–sea exchange of carbon dioxide (CO₂) in the North Sea are investigated using the three-dimensional coupled physical–biogeochemical model ECOHAM (ECOLOGICAL-model, HAMBURG). We validate our simulations using field data for the years 2001–2002 and identify the controls of the air–sea CO₂ flux for two locations representative for the North Sea's biogeochemical provinces. In the seasonally stratified northern region, net CO₂ uptake is high (2.06 mol m⁻² a⁻¹) due to high net community production (NCP) in the surface water. Overflow production releasing semi-labile dissolved organic carbon needs to be considered for a realistic simulation of the low dissolved inorganic carbon (DIC) concentrations observed during summer. This biologically driven carbon drawdown outcompetes the temperature-driven rise in CO₂ partial pressure (pCO₂) during the productive season. In contrast, the permanently mixed southern region is a weak net CO₂ source (0.78 mol m⁻² a⁻¹). NCP is generally low except for the spring bloom because remineralization parallels primary production. Here, the pCO₂ appears to be controlled by temperature.

© 2009 Elsevier Ltd. All rights reserved.

1. Introduction

The role of coastal shelf seas in the exchange of CO₂ between atmosphere and ocean has been in the focus of many investigations over the past few years (Borges, 2005). Despite evidence of the shelf seas' significant contribution, global estimates of current and future ocean carbon uptake often neglect shelf areas (e.g. Takahashi et al., 2009). The North Sea and other shelf seas have been identified as continental shelf pumps, transferring atmospheric CO₂ into the ocean interior via physical and/or biological mechanisms (e.g. Tsunogai et al., 1999; Thomas et al., 2004; Borges et al., 2005). The mechanisms of this CO₂ uptake and their seasonality, however, are still poorly understood.

The North Sea constitutes of two biogeochemical provinces (Thomas et al., 2004): In the shallow southern North Sea, biological uptake and release of dissolved inorganic carbon (DIC) occur in a single compartment with a mixed water column throughout the year. As a result, after the initial DIC drawdown during the spring phytoplankton bloom the DIC remains at

intermediate levels throughout the mixed water column (Fig. 1). In the seasonally stratified northern part, primary production draws down DIC in the surface mixed layer. Organic material sinks into the subsurface layer where remineralization releases DIC with no contact to the atmosphere. Low DIC levels prevail in the surface layer, while the DIC-enriched deeper waters are exported to the adjacent North Atlantic. In fall, mixing and remineralization restore uniform high winter DIC levels in both regions (Bozec et al., 2006). Weak annual net air–sea CO₂ fluxes have been reported for the southern regions, while the North has been identified as a strong sink for atmospheric CO₂ (Thomas et al., 2004).

In this study, we unravel the biogeochemical dynamics controlling the air–sea CO₂ fluxes in detail for two representative locations in the North Sea employing a three-dimensional coupled physical–biogeochemical ecosystem model.

2. Methods

2.1. The model

We use the three-dimensional ecosystem model ECOHAM (ECOLOGICAL-model, HAMBURG; Pätsch and Kühn, 2008), consisting of a biogeochemical model coupled to the hydrodynamical

* Corresponding author at: IFM-GEOMAR, Leibniz Institute of Marine Sciences at the University of Kiel, Düsterbrookweg 20, 24105 Kiel, Germany. Tel.: +49 431 600 4032. E-mail address: fprowe@ifm-geomar.de (A.E.F. Prowe).

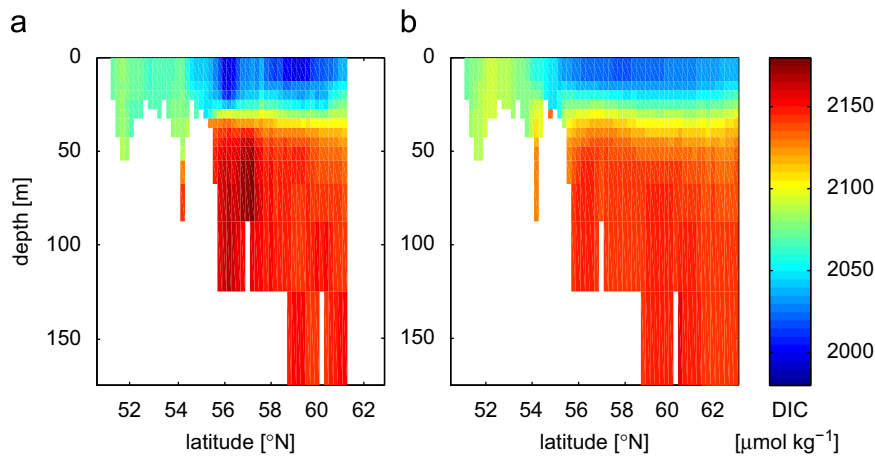


Fig. 1. Observed (a) and simulated (b) monthly mean DIC ($\mu\text{mol kg}^{-1}$) along a section at 2°E in August/September 2001.

HAMBURG Shelf Ocean Model (HAMSOM; Backhaus, 1985; Pohlmann, 1996). Simulations for the years 2001–2002 comprise carbon (C), nitrogen (N) and oxygen cycles including state variables DIC, total alkalinity (TA), bulk phytoplankton, bulk zooplankton, bacteria, detritus and dissolved organic matter (DOM).

DIC is calculated prognostically while TA is restored to yield daily values. A relaxation time of 14 days allows for short-term variability. Restoring (TA) and initial values (DIC and TA) within the North Sea are taken from observational data (Thomas et al., 2005, 2009) obtained during four cruises in August/September 2001, November 2001, February 2002 and May 2002 at 97 stations on a $1^\circ \times 1^\circ$ grid (see Thomas, 2002 for details). For the adjacent regions of the North Atlantic, DIC initial and boundary conditions are taken from CDIAC (Carbon Dioxide Information Analysis Center: www.cdiac.ornl.gov; data from NDP 076). Here, above 100 m water depth DIC values are derived using the T – S –nitrate correlation proposed by Lee et al. (1999) with T , S and nitrate data from Conkright et al. (2002). The latter data are also used as boundary conditions for nitrate. TA initial and restoring values for the adjacent North Atlantic are taken from CDIAC NDP 076. For all other state variables, reflecting boundary conditions are used because of the lack of sufficient data. The model is forced by six-hourly wind stress, air pressure and temperature, humidity, cloudiness and six-hourly short wave radiation recalculated to two-hourly resolution. Data stem from the ERA-40 reanalysis data provided by the European Centre for Medium-Range Weather Forecasts with a spatial resolution of 1.125° (ECMWF, 2005). River inputs of DIC, particulate organic C and N, nitrate and ammonium are taken from Pätsch and Lenhart (2004) as daily data for the German, Dutch and Belgian rivers. For the Scandinavian and British river loads, data from Heath et al. (2005) representing annual loads of the year 1990 are used.

In the model, C- and N-cycles are coupled via several fixed C/N-ratios for phytoplankton, zooplankton and bacteria. Detritus and DOM have flexible C/N-ratios, since the C and N contents are simulated independent from each other.

2.2. Overflow production

Shifts in environmental factors such as light and nutrients can cause the excretion of organic carbon from phytoplankton cells (Mague et al., 1980). This extracellular release of organic carbon leads to the formation of high molecular dissolved organic matter with a negligible content of nitrogen (“overflow production”,

Fogg, 1983). This enhanced exudation of DOC is often observed when inorganic nutrients become depleted but photosynthesis continues. The excess DIC uptake without corresponding nutrient uptake is therefore also referred to as “carbon overconsumption” (Toggweiler, 1993), and facilitates a non-Redfield pathway for carbon fixation. As physiological basis, e.g. Geider and MacIntyre (2002) discuss the glycolate metabolism as a means of reducing oxidative stress at high irradiance (Kozaki and Takeba, 1996) due to photorespiration.

For the fate of the extracellular DOC from overflow production two pathways are discussed (Schartau et al., 2007). The excess DIC can be transferred to the labile DOC pool which is taken up by bacteria (e.g. Kähler and Koeve, 2001). Alternatively, a fraction of the exuded DOC consisting of polysaccharides can fuel the formation of transparent exopolymer particles (TEP; Mopper et al., 1995; Zhou et al., 1998). For *Phaeocystis* colonies, for instance, fixation of carbon well above the Redfield ratio is linked to increased production of mainly polysaccharidic mucilaginous matrix under low nutrient, high light conditions (see Bozec et al., 2006 and references therein), which again may lead to enhanced TEP formation (Mari et al., 2005). Field observations in various areas including the Northeast Atlantic and the English Channel show that the increase of DOC during the productive season significantly exceeds the corresponding DON increase multiplied by the Redfield ratio (Williams, 1990; Kähler and Koeve, 2001). The two pathways have different implications for export of carbon from the upper ocean depending on which form of carbon, DOC vs. POC, is finally produced.

This study intends to elucidate whether non-Redfield processes need to be taken into account for (future) modelling studies in highly dynamic ocean regions like shelf seas. Consequently, for this application C and N uptake by phytoplankton are decoupled to permit overflow production of C-rich, N-deplete DOM, while the formulation is deliberately kept simple.

Total net primary production (flux dic_phc) consists of a Redfield-based portion (NPP_{red} ; flux dic_phc_{red}) and the overflow production (flux dic_phc_{exc})

$$dic_phc = dic_phc_{red} + dic_phc_{exc} \quad (1)$$

Nutrient-limited primary production is applied in both the phytoplankton C and N equations of state, applying the Redfield ratio for conversion between C and N units. It is formulated as Michaelis–Menten equation for two nutrients

$$dic_phc_{red} = T_{fac} \cdot F_{light} \cdot v_P \cdot (Q_1 + Q_2) \cdot phc, \quad (2)$$

Table 1
Selected parameters of the biogeochemical model and their values.

Description	Parameter	Value	Unit
Remineralization rate benthic carbon	<i>brc</i>	1.00	d ⁻¹
Remineralization rate benthic nitrogen	<i>brn</i>	0.85	d ⁻¹
Breakdown rate of <i>soc</i> to <i>doc</i>	δ_{soc}	0.0037	d ⁻¹
Overflow production	<i>f_{exc}</i>	0–1	
Light dependency phytoplankton growth	<i>F_{light}</i>	0–1	
Half-saturation constant nitrate uptake	<i>K₁</i>	0.5	mmol N m ⁻³
Half-saturation constant ammonium uptake	<i>K₂</i>	0.05	mmol N m ⁻³
Breakdown rate slowly sinking detritus	μ_4	0.03	d ⁻¹
Breakdown rate fast sinking detritus	μ_5	0.01	d ⁻¹
Temperature dependency phytoplankton growth	<i>T_{fac}</i>	$1.5^{(T-T_0)/T_0}$	$T_0 = 10^\circ\text{C}$
Maximum phytoplankton growth rate	<i>v_p</i>	1.1	d ⁻¹
Sinking velocity slowly sinking detritus	<i>w_{d1}</i>	0.1	m d ⁻¹
Sinking velocity fast sinking detritus	<i>w_{d2}</i>	1.0	m d ⁻¹

All rates are valid for 10 °C. The full set of model equations and parameters can be found in Pätzsch and Kühn (2008).

where

$$Q1 = \frac{\frac{n3n}{K_1}}{1 + \frac{n3n}{K_1} + \frac{n4n}{K_2}} \quad \text{and} \quad Q2 = \frac{\frac{n4n}{K_2}}{1 + \frac{n3n}{K_1} + \frac{n4n}{K_2}}$$

describe limitation of primary production by nitrate (*n3n*) and ammonium (*n4n*) availability, respectively. *phc* is the phytoplankton concentration, *T_{fac}* and *F_{light}* · *v_p* are the temperature factor and the light-dependent phytoplankton growth rate, respectively (see Table 1 and Pätzsch and Kühn, 2008 for model equations and parameter values).

Similar to Anderson and Williams (1998) and Smith et al. (2005), the excess primary production is formulated as fraction *f_{exc}* of the difference between production limited by both nutrients and light and nutrient-saturated, only light-limited production (Bratbak and Thingstad, 1985)

$$dic_phc_{exc} = f_{exc} \cdot (1 - (Q1 + Q2)) \cdot T_{fac} \cdot F_{light} \cdot v_p \cdot phc. \quad (3)$$

This overflow production is immediately released from the algal cells as semi-labile organic carbon (*soc*; flux *phc_{soc}*). It is then degraded to labile DOC (flux *soc_{doc}*) available to bacteria at a rate δ_{soc} corresponding to degradation on time scales of three months:

$$\frac{\partial soc}{\partial t} = phc_soc - soc_doc = dic_phc_{exc} - \delta_{soc} \cdot soc. \quad (4)$$

It does not increase phytoplankton biomass and constitutes a carbon flux outside the Redfield-coupled C and N fluxes in the model. This formulation represents the first pathway for extracellular organic carbon produced by overflow production. TEP formation, although likely to be of significance (Schartau et al., 2007), is omitted for the benefit of simplicity.

2.3. Analysis

Net community production (NCP) is the difference between simulated net primary production (NPP) and heterotrophic pelagic and benthic respiration (*R*): $NCP = NPP - R$. The *pCO₂* is calculated from simulated DIC and TA. We decompose the variability of the ΔpCO_2 ($pCO_{2,sea} - pCO_{2,air}$) into the variabilities induced by variations of surface DIC, TA, temperature (*T*) and salinity (*S*): the simulated ΔpCO_2 is recalculated as function of each individual property varying over time *t*, while the other three

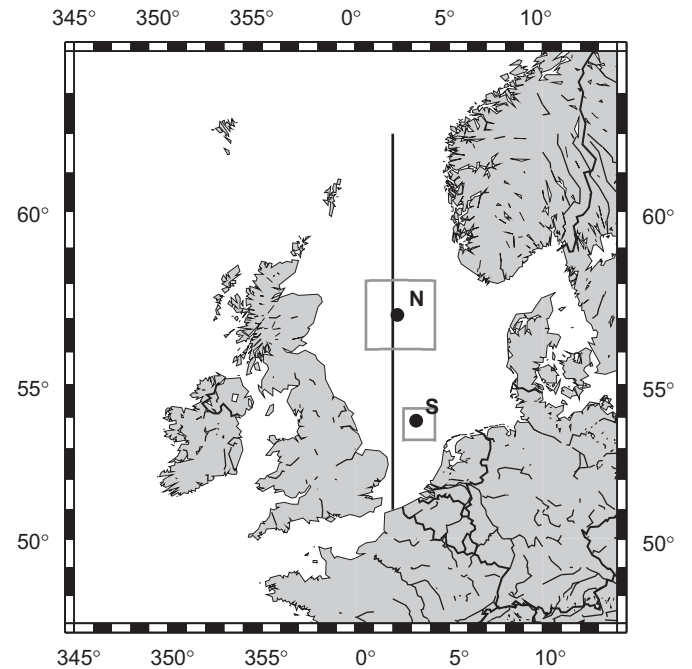


Fig. 2. The model domain including the North Sea, showing the section along 2° E (cf. Fig. 1), location N (57.1° N, 2.25° E) and location S (53.9° N, 3.25° E). The gray boxes show the areas used for spatial averages of DIC and ΔpCO_2 in Figs. 5 and 6.

are held constant ($t_0 = \text{January 1}$), e.g.

$$\delta pCO_2(DIC) = \Delta pCO_2(DIC_t, TA_{t_0}, T_{t_0}, S_{t_0}). \quad (5)$$

Two three-dimensional simulations with and without overflow production each including three spin-up years were performed with the coupled model. We assess model performance by comparing three crucial parameters of the C system, DIC, *pCO₂* and temperature, to observational data from four cruises in August/September 2001, November 2001, February 2002 and May 2002 (see Thomas et al., 2005; Bozec et al., 2006 for details). The study focuses on two locations representative for conditions in the northern (57.1° N, 2.25° E, location N) and southern North Sea (53.9° N, 3.25° E, location S; Fig. 2) to investigate the drivers of the air–sea *CO₂* flux, in particular vertical water column structure, rather than providing budgets at the basin-wide scale. The two locations are chosen at a distance from the coast in order not to be affected by river inputs, and close to observational stations to ensure comparability between simulations and observations. They provide windows to the North Sea biogeochemical system for assessing model results in detail before analyzing the air–sea *CO₂* flux in the southern and northern North Sea.

3. Results and discussion

3.1. Model assessment

Near-surface temperature (*T*) is well captured by the model (Figs. 3–5) with the exception of August/September at location N (Fig. 5b). The simulated monthly mean and in situ *T* at the day of observation are 2 and 1.5 °C lower than observed, respectively. These differences might reflect biases in the ERA-40 air temperature forcing. Also, at this time the simulated vertical temperature gradient in the water column is smaller than observed (Fig. 4g). In spring, *T* at both locations is simulated correctly, but the water column is more strongly stratified

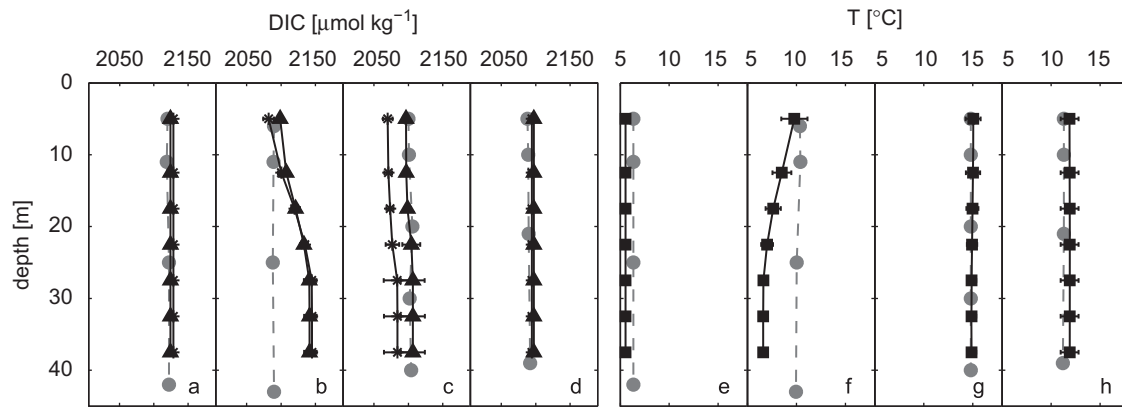


Fig. 3. Simulated dissolved inorganic carbon (DIC; $\mu\text{mol kg}^{-1}$) (a–d) and temperature (T [°C]) (e–h) profiles compared to observations (gray dots) at location S (53.9° N, 3.25° E) for (a, e) February 2001, (b, f) May 2001, (c, g) August/September 2001, (d, h) November 2001. Simulated values are monthly means with error bars indicating one temporal standard deviation. DIC is shown for two cases, allowing non-Redfield overflow production (squares) and primary production coupled to nutrient availability via the Redfield ratio (triangles). Simulations for February and May 2001 are compared to observations from cruises in 2002 as guidelines.

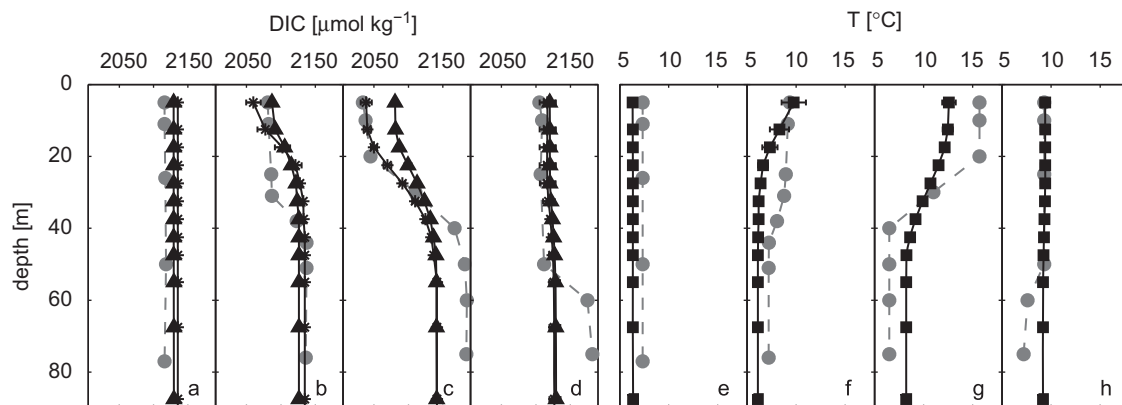


Fig. 4. Simulated dissolved inorganic carbon (DIC; $\mu\text{mol kg}^{-1}$) (a–d) and temperature (T [°C]) (e–h) profiles compared to observations (gray dots) at location N (57.1° N, 2.25° E) for (a, e) February 2001, (b, f) May 2001, (c, g) August/September 2001, (d, h) November 2001. Simulated values are monthly means with error bars indicating one temporal standard deviation. DIC is shown for two cases, allowing non-Redfield overflow production (squares) and primary production coupled to nutrient availability via the Redfield ratio (triangles). Simulations for February and May 2001 are compared to observations from cruises in 2002 as guidelines.

compared to the observations (Figs. 3f and 4f). T values < 0.5 °C lower than observed in February (Fig. 5d) are within the accuracy of circulation models (e.g. Pohlmann, 2006). More details on the circulation model can be found in Pohlmann (1996, 2006).

The simulations successfully reproduce the observed DIC patterns in both the southern and northern North Sea (Figs. 1, 3–5). Two biogeochemical provinces are well distinguished: in the deeper North (54.5–61° N) a vertical DIC gradient establishes in summer because of biological drawdown and stratification, whereas the shallow South (51–54.5° N) is characterized by a vertically homogeneous distribution (Figs. 1, 3 and 4).

Simulated surface and mixed-layer DIC levels are most sensitive to the strength of overflow production. At location N, the simulation with Redfield-based primary production (NPP_{red}) considerably overestimates summer surface DIC levels by approx. $40 \mu\text{mol kg}^{-1}$ (Fig. 5c). At this time, primary production is limited by inorganic nutrients, therefore the underestimated mixed-layer temperature (Fig. 4g) alone cannot explain such high simulated DIC levels. Observed lower DIC levels can be reproduced both in magnitude and seasonality by permitting overflow production ($f_{\text{exc}} = 0.75$). In contrast, at location S, NPP_{red} ($f_{\text{exc}} = 0$) reproduces observed DIC levels at all depths very well (Figs. 3a–d and 5a), while permitting overflow production underestimates summer DIC levels. In agreement with observational results comparing

C-based NCP and NCP estimated by converting nutrient data using the Redfield ratio for the same area and time (Bozec et al., 2006), we take overflow production into account for the northern regions only (north of 54.5° N).

Simulated DIC values are higher than observed in winter in particular at location N (Fig. 5c). As the seasonal cycle of DIC is well captured and subsurface DIC levels in summer are lower than observed (Fig. 4c and d), vertical transport of C from deeper layers during fall/winter appears not to be the main cause. Thus the overestimation likely reflects high DIC restoring values at the model boundaries. Given continued uptake of DIC despite inorganic nutrient limitation, the stronger stratification (Fig. 4f and g) in the model leads to an overall shallower mixed layer and might result in lower annual primary production and less vertical export via sinking organic matter. Underestimated sinking would also explain the low simulated DIC concentrations below the mixed layer (Fig. 4c). The applied sinking velocities (Table 1; Pätzsch and Kühn, 2008) are identical with values used by Fennel et al. (2006) for the Middle Atlantic Bight, and are low compared to other studies (e.g. Pätzsch et al., 2002). In addition, TEP formation from exuded DOM, which constitutes the second pathway for overflow production (Schartau et al., 2007), might induce enhance sinking and lead to additional C export to the subsurface layer. However, since the simulated nitrate profiles are overestimated compared to the observations (not shown), it is

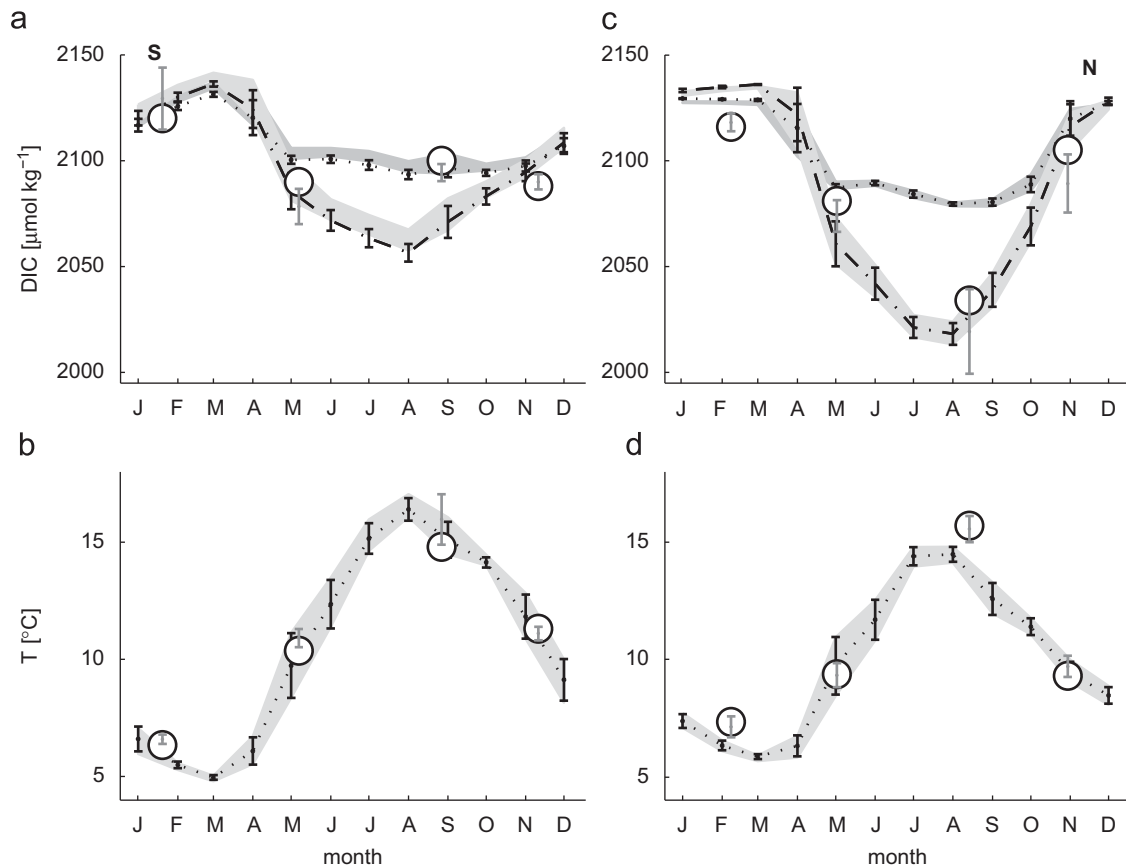


Fig. 5. Simulated surface dissolved inorganic carbon (DIC; $\mu\text{mol kg}^{-1}$) at location S (53.9°N, 3.25°E); (a) and location N (57.1°N, 2.25°E); (b) for Redfield primary production (dotted line) and non-Redfield overflow production (dash-dotted line). Simulated near-surface temperatures ($T^{\circ}\text{C}$) (dotted line) at location S (c) and location N (d). Simulations for 2001 are compared to observations (open circles) at two stations from cruises in August/September and November 2001, and February and May 2002 as guidelines. Simulated values are monthly means averaged over a $1^{\circ} \times 1^{\circ}$ area corresponding to these stations, with black error bars indicating one spatial standard deviation. Gray error bars indicate spatial averages \pm one standard deviation of three and nine observational stations in the southern and northern North Sea, respectively (cf. Fig. 2). Gray shaded areas show the corresponding averages \pm one standard deviation of the model data.

also likely that the model simulates water masses with a different biogeochemical signature entering from the outer shelf/North Atlantic area across the northern boundary of the North Sea. Sensitivity studies investigating the effect of different sinking velocities for organic matter as well as different remineralization rates show only small variations in DIC, ΔpCO_2 and air–sea CO_2 flux in general, and in particular compared to the effect of changing the degree of overflow production.

At location S, DIC levels after the spring bloom are slightly higher than observed (Fig. 5a, dotted line). During spring, the simulated DIC gradient from low surface levels to winter levels at depth contrasts the observed uniform low DIC profile (Fig. 3b), in consequence of the similar, but reversed temperature gradient (Fig. 3f). The corresponding observations show that the water column was well mixed and the biologically mediated drawdown of DIC affected the entire water column. The simulated stronger stratification at this time of the year might lead to an underestimated spring bloom DIC drawdown and cause the slightly higher than observed DIC levels.

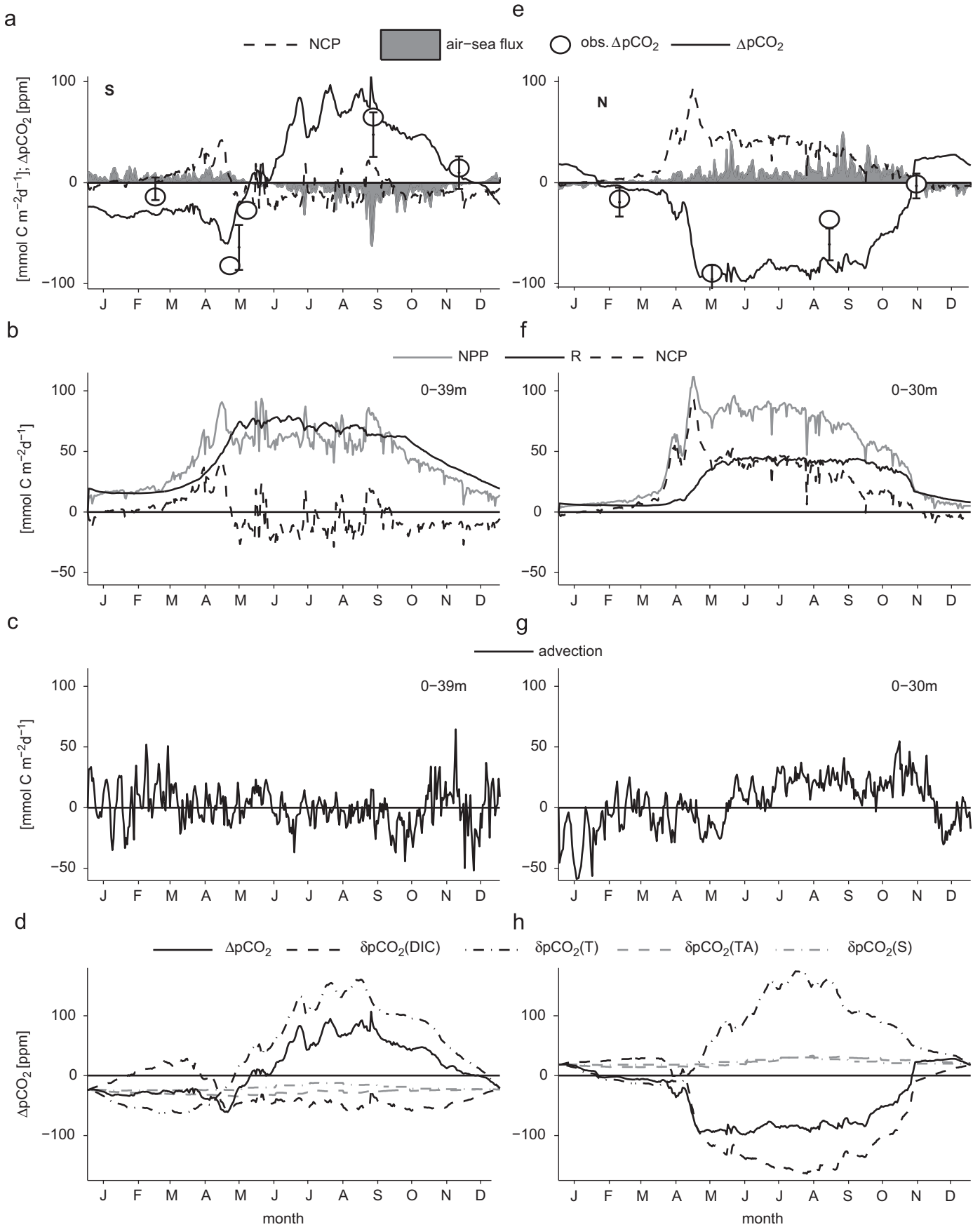
The simulated ΔpCO_2 (Fig. 6a and e) agrees well with observations in both magnitude and seasonal cycle, further confirming the distinction between NPP_{red} at location S, and overflow production at location N. It underestimates the observed ΔpCO_2 in summer at location N and in winter at location S because of lower than observed T. Overestimated ΔpCO_2 values in winter at location N and in spring at location S reflect higher than observed DIC.

3.2. pCO_2 and air–sea CO_2 exchange

3.2.1. Southern North Sea

In the southern North Sea, NPP_{red} is high from the spring bloom in March/April until fall, and low during winter (Fig. 6b). It is lower than R throughout the year except for the period of the spring bloom and isolated events during summer. With carbon fixation strictly coupled to inorganic nutrient availability, remineralization within the mixed water column and the sediment sustains a constantly high level of regenerated primary production throughout the season.

As a result, NCP is positive only during the spring bloom, and the annual NCP of $-1.01 \text{ mol C m}^{-2} \text{ a}^{-1}$ classifies the water column as weakly heterotrophic: remineralization of organic carbon exceeds uptake of inorganic carbon. The surplus organic matter required to sustain the heterotrophic status is supplied by advection from river inputs, the coastal regions, and the North Atlantic via the English Channel. Other studies estimate an autotrophic state for the southern North Sea (Bozec et al., 2006) and the Southern Bight (Schiettecatte et al., 2007), in the latter case because of a stronger spring bloom. Near-shore areas such as the Belgian coastal zone have been estimated as net heterotrophic (Borges and Frankignoulle, 2002; Borges et al., 2008). The simulated NPP_{red} of $191.5 \text{ g C m}^{-2} \text{ a}^{-1}$ is in the lower range of observed primary production (Joint and Pomroy, 1993; Reid et al., 1990), which usually shows high interannual variability (Borges et al., 2008). A higher C uptake during the spring bloom would



increase primary production and might shift NCP values towards autotrophy.

Surface waters are characterized by CO_2 undersaturation in winter (Fig. 6a), a short, but significant pCO_2 decrease in spring and an increase to strong supersaturation during summer and fall. Changes in DIC ($\delta\text{pCO}_2(\text{DIC})$, Fig. 6d) dominate the ΔpCO_2 only during November to April: in spring, the positive NCP causes the DIC drawdown; in winter, DIC levels mainly increase due to remineralization in November/December ($\text{NCP} < 0$) or advective and atmospheric inputs in February/March ($\text{NCP} > 0$, Fig. 6c). However, a strong net effect of advective DIC transport on the DIC concentration cannot be identified: the net change in concentration within the surface layer due to advective transport is $-0.07 \text{ mmol C m}^{-2} \text{ d}^{-1}$. In the absence of strong biological DIC uptake ($\text{NCP} \approx 0$) during the remainder of the year the ΔpCO_2 signal is dominated by the effects of temperature ($\delta\text{pCO}_2(T)$), leading to CO_2 supersaturation and release of CO_2 to the atmosphere in summer and fall. During winter, decreasing temperatures eventually result in CO_2 uptake (Fig. 6a and d). Benthic calcification as driver of the ΔpCO_2 , as suggested by Borges and Frankignoulle (2003) for the English Channel, would decrease TA and lead to a net release of CO_2 to surrounding water. Since the observed TA is used for restoring, any potential effect is implicitly included in the model. For this location, benthic calcification does not seem to be of importance in driving the air–sea CO_2 flux.

At the annual scale, $0.78 \text{ mol C m}^{-2} \text{ a}^{-1}$ are released to the atmosphere. This value is the result of a delicate balance between the strength of net carbon fixation, i.e. NCP, and the dominating temperature effect. Close to neutral air–sea CO_2 exchange has been reported by other studies (Thomas et al., 2004; Schiettecatte et al., 2007; Borges et al., 2008), partly with opposing, yet weak fluxes. Recent studies also show interannual variability of the NCP and air–sea CO_2 exchange (Borges et al., 2008). These ambiguous findings could be due to the fact that governing processes balance closely and the net CO_2 flux is small, which is confirmed by all studies. In the present study, this balance is robust over a range of primary production levels simulated in sensitivity runs.

3.2.2. Northern North Sea

In the upper 0–30 m of the northern North Sea, simulated primary production increases sharply during the spring bloom (Fig. 6f). After inorganic nutrients are exhausted, primary production recedes with overflow production constituting approx. 50% of total NPP during summer, or 34% at the annual scale. About 60% of the annual primary production are respired in the surface layer. The remaining organic material mostly sinks out of the surface layer. A smaller amount of DIC is supplied by advection during summer (Fig. 6g), which further stresses the importance of biological mechanisms for the DIC drawdown as opposed to physical transport. With an average daily flux of $4.62 \text{ mmol C m}^{-2} \text{ d}^{-1}$ over the year, however, the net change in concentration due to advection is small. The resulting surface layer NCP is strongly positive throughout the productive season from April until September until mixing starts in fall. NCP peaks during the spring bloom, when respiration lags behind primary production by approx. two weeks. The simulated annual primary production of $205 \text{ g C m}^{-2} \text{ a}^{-1}$ ($135 \text{ g C m}^{-2} \text{ a}^{-1}$ NPP_{red} only) is well

within the range of observations of $119\text{--}200 \text{ g C m}^{-2} \text{ a}^{-1}$ (Reid et al., 1990; Joint and Pomroy, 1993) considering that these field studies do not account for overflow production.

The net annual NCP is sensitive to the strength of overflow production. The simulated value of $8.01 \text{ mol C m}^{-2} \text{ a}^{-1}$ ($f_{\text{exc}} = 0.75$, 0–30 m) exceeds comparable observation-based NCP estimates (Bozec et al., 2006). Comparing primary production (PP) levels proves difficult because of limitations and differences in methods estimating production from field observations (Gazeau et al., 2004), and scarcity of adequate data for the North Sea. In particular, the ^{14}C method has inherent conceptual problems since it gives estimates which are intermediate between gross primary production (for short incubations) and net primary production (for long incubations, e.g. Peterson, 1980; Marra, 2002). Furthermore, ^{14}C -based primary production yields results for particulate phytoplankton production only and does not account for dissolved products, e.g. from overflow production. Dissolved PP products have been found a significant part of total PP, and are estimated to account for up to 20% for oligotrophic oceanic (Morán et al., 2002) as well as eutrophic coastal (Marañón et al., 2004) regions. Since in the model all overflow production remains within the DOC pool, the simulated overflow production also contains a potential particulate fraction created by TEP formation. It is therefore likely to exceed these estimates of only dissolved PP products. Sensitivity runs with a lower percentage of overflow production give lower NCP values closer to other estimates, but overestimate the observed DIC. Since DIC concentrations are affected via both sinking and remineralization rates of POC and DOC, further work is needed, also concerning the fate of DOC from overflow production in the model, to reliably capture the ratio of dissolved and particulate PP.

The ΔpCO_2 is characterized by strongly undersaturated levels during the spring bloom, when NCP is highest (Fig. 6e). Throughout the productive season, ΔpCO_2 remains strongly undersaturated at nearly constant levels until the onset of mixing in fall, in contrast to the shallow southern North Sea. The constantly low ΔpCO_2 results from a biologically ($\text{NCP} > 0$) driven DIC drawdown, which counteracts the effect of rising temperature on the ΔpCO_2 (Fig. 6h). This DIC drawdown is facilitated by overflow production overcoming inorganic nutrient limitation. Sinking of organic matter and slow degradation rates of semi-labile DOC maintain DIC and thus ΔpCO_2 conditions until the onset of mixing in fall.

At the annual scale, $2.06 \text{ mol C m}^{-2} \text{ a}^{-1}$ CO_2 are taken up from the atmosphere at location N, which slightly exceeds an uptake of $1.64 \text{ mol C m}^{-2} \text{ a}^{-1}$ estimated from observations (Thomas et al., 2005).

4. Conclusions

The air–sea CO_2 flux in the two biogeochemical provinces of the North Sea is the result of a balance between temperature and biological effects, which strongly depend on the stratification and its consequences for the fate of biological production. In the southern North Sea, primary production over long periods relies on recycled nutrients, preventing high net C fixation. Temperature, and to a certain degree degradation of allochthonous organic matter become the seemingly dominant drivers of the air–sea CO_2

Fig. 6. (a, e) Simulated and observed ΔpCO_2 (ppm), net community production (NCP) and air-to-sea CO_2 flux ($\text{mmol C m}^{-2} \text{ d}^{-1}$) (positive: CO_2 uptake from the atmosphere), (b, f) NCP, net primary production (NPP) and respiration (R; zooplankton, bacteria and benthos), (c, g) sum of horizontal and vertical advective fluxes (running average), at location S and location N in the southern and northern North Sea, respectively, in 2001. Variables are given for the entire water column (a–c; 0–39 m) at location S and for an upper layer (e–g; 0–30 m) at location N. Two observations in May at location S are two passes of the same $1' \times 1'$ area 15 days apart. Error bars indicate spatial averages \pm one standard deviation of the observed ΔpCO_2 within the same areas used in Fig. 5 (cf. Fig. 2). Mean net advective fluxes are $-0.07 \text{ mmol C m}^{-2} \text{ d}^{-1}$ (location S) and $4.62 \text{ mmol C m}^{-2} \text{ d}^{-1}$ (location N). (d, h) The simulated ΔpCO_2 is recalculated as function of one varying property out of surface dissolved inorganic carbon (DIC; e.g. $\delta\text{pCO}_2(\text{DIC})$), total alkalinity (TA), temperature (T) and salinity (S), while the other three are held constant at their value of January 1.

flux. In the northern North Sea, stratification of the water column permits export of organic matter out of the surface layer. Overflow production under inorganic nutrient limitation facilitates continued net carbon fixation counteracting the temperature-driven $\Delta p\text{CO}_2$ increase during summer. The subsurface water masses are enriched in DIC by remineralization, which can then be exported into the North Atlantic, forcing CO_2 replenishment from the atmosphere. Our model results indicate the importance of C overconsumption and dissolved products of primary production in driving CO_2 fluxes. More investigations are needed, however, to unravel their seasonality and mechanisms under different oceanic conditions.

Acknowledgments

We are grateful to Drs. Pohlmann, Lenhart and Ebenhöf for constructive discussions and encouragement. F.P. gratefully acknowledges financial support by Dr. Peter Schaefer. This work benefited from comments by Joe Salisbury and one anonymous reviewer. H.T. holds a Canada research chair. A.V.B. is a research associate at the FNRS. This work contributes to CARBOOCEAN (EU-FP6), IGBP-IHDP LOICZ and EU CSA COCOS (212196).

References

- Anderson, T.R., Williams, P.J. Le B., 1998. Modelling the seasonal cycle of dissolved organic carbon at station E₁ in the English Channel. *Estuarine, Coastal and Shelf Science* 46, 93–109.
- Backhaus, J.O., 1985. A three-dimensional model for the simulation of shelf sea dynamics. *Deutsche Hydrographische Zeitung* 38 (4), 165–187.
- Borges, A.V., 2005. Do we have enough pieces of the jigsaw to integrate CO_2 fluxes in the coastal ocean?. *Estuaries* 28 (1), 3–27.
- Borges, A.V., Delille, B., Frankignoulle, M., 2005. Budgeting sinks and sources of CO_2 in the coastal ocean: diversity of ecosystems counts. *Geophysical Research Letters* 32, L14601 10.1029/2005GL023053.
- Borges, A.V., Frankignoulle, M., 2002. Distribution and air–water exchange of carbon dioxide in the Scheldt plume off the Belgian coast. *Biogeochemistry* 59 (1–2), 41–67.
- Borges, A.V., Frankignoulle, M., 2003. Distribution of surface carbon dioxide and air–sea exchange in the English Channel and adjacent areas. *Journal of Geophysical Research* 108 (C5), 3140 10.1029/2000JC000571.
- Borges, A.V., Ruddick, K., Schiettecatte, L.-S., Delille, B., 2008. Net ecosystem production and carbon dioxide fluxes in the Scheldt estuarine plume. *BMC Ecology* 8, 15, doi:10.1186/1472-6785-8-15.
- Bozec, Y., Thomas, H., Schiettecatte, L.-S., Borges, A.V., Elkalay, K., de Baar, H.J.W., 2006. Assessment of the processes controlling seasonal variations of dissolved inorganic carbon in the North Sea. *Limnology and Oceanography* 51 (6), 2746–2762.
- Bratbak, G., Thingstad, T.F., 1985. Phytoplankton–bacteria interactions: an apparent paradox? Analysis of a model system with both competition and commensalism. *Marine Ecology Progress Series* 25, 23–30.
- Conkright, M.E., Locarnini, R.A., Garcia, H.E., O'Brien, T.D., Boyer, T.P., Stephens, C., Antonov, J.I., 2002. *World Ocean Atlas 2001: Objective Analyses, Data Statistics, and Figures*. CD-ROM Documentation. National Oceanographic Data Center, Silver Spring, MD, 17pp.
- ECMWF, 2005. European Centre for Medium-Range Weather Forecasts, Re-Analysis ERA-40 online dataset <<http://www.ecmwf.int>>.
- Fennel, K., Wilkin, J., Levin, J., Moisan, J., O'Reilly, J., Haidvogel, D., 2006. Nitrogen cycling in the Middle Atlantic Bight: results from a three-dimensional model and implications for the North Atlantic nitrogen budget. *Global Biogeochemical Cycles* 20, GB3007, doi:10.1029/2005GB002456.
- Fogg, G.E., 1983. The ecological significance of extracellular products of phytoplankton photosynthesis. *Botanica Marina* 26 (1), 3–14.
- Gazeau, F., Smith, S.V., Gentili, B., Frankignoulle, M., Gattuso, J.-P., 2004. The European coastal zone: characterization and first assessment of ecosystem metabolism. *Estuarine, Coastal and Shelf Science* 60, 673–694.
- Geider, R.J., MacIntyre, H.L., 2002. Physiology and biochemistry of photosynthesis and algal carbon acquisition. In: le B. Williams, P.J., Thomas, D.N., Reynolds, C.S. (Eds.), *Phytoplankton Productivity: Carbon Assimilation in Marine and Freshwater Ecosystems*. Blackwell Science, Oxford, pp. 44–77.
- Heath, M.R., Pätsch, J., Edwards, A., Turrell, W.R., Greathead, C., Davies, I.M., 2005. Modelling the behaviour of nutrients in the coastal waters of Scotland—an update on inputs from Scottish aquaculture and their impact on eutrophication status. *Fisheries Research Service Report* 10/02.
- Joint, I., Pomroy, A., 1993. Phytoplankton biomass and production in the southern North Sea. *Marine Ecology Progress Series* 99, 169–182.
- Kähler, P., Koeve, W., 2001. Marine dissolved organic matter: can its C:N ratio explain carbon overconsumption. *Deep-Sea Research I* 48, 49–62.
- Kozaki, A., Takeba, G., 1996. Photorespiration protects C₃ plants from photooxidation. *Nature* 384, 557–560 10.1038/384557a0.
- Lee, K., Wanninkhof, R., Feely, R.A., Millero, F.J., Peng, T.-H., 1999. Global distribution of total inorganic carbon in surface water. In: Nojiri, Y. (Ed.), *Proceedings of the 2nd International Symposium CO₂ in the Oceans*, Tsukuba, pp. 493–496.
- Mague, T.H., Friberg, E., Hughes, D.J., Morris, I., 1980. Extracellular release of carbon by marine phytoplankton; a physiological approach. *Limnology and Oceanography* 25 (2), 262–279.
- Marañón, E., Cermeño, P., Fernández, E., Rodríguez, J., Zabala, L., 2004. Significance and mechanisms of photosynthetic production of dissolved organic carbon in a coastal eutrophic ecosystem. *Limnology and Oceanography* 49 (5), 1652–1666.
- Mari, X., Rassoulzadegan, F., Brussaard, C.P.D., Wassmann, P., 2005. Dynamics of transparent exopolymeric particles (TEP) production by *Phaeocystis globosa* under N- or P-limitation: a controlling factor of the retention/export balance. *Harmful Algae* 4, 895–914.
- Marra, J., 2002. Approaches to the measurement of plankton production. In: Williams, P., Thomas, D., Reynolds, C. (Eds.), *Phytoplankton Productivity*. Blackwell Science, Oxford, pp. 78–108.
- Mopper, K., Zhou, J., Ramana, K.S., Passow, U., Dam, H.G., Drapeau, D.T., 1995. The role of surface-active carbohydrates in the flocculation of a diatom bloom in a mesocosm. *Deep-Sea Research II* 42 (1), 47–73.
- Morán, X.A.G., Estrada, M., Gasol, J.M., Pedrós-Alió, C., 2002. Dissolved primary production and the strength of phytoplankton–bacterioplankton coupling in contrasting marine regions. *Microbial Ecology* 44, 217–223 10.1007/s00248-002-1026-z.
- Pätsch, J., Kühn, W., 2008. Nitrogen and carbon cycling in the North Sea and exchange with the North Atlantic—a model study. Part I. Nitrogen budget and fluxes. *Continental Shelf Research* 28, 767–787.
- Pätsch, J., Kühn, W., Radach, G., Santana Casiano, J.M., Gonzalez Davila, M., Neuer, S., Freudenthal, T., Llinas, O., 2002. Interannual variability of carbon fluxes at the North Atlantic station ESTOC. *Deep-Sea Research II* 49, 253–288.
- Pätsch, J., Lenhart, H.-J., 2004. Daily loads of nutrients, total alkalinity, dissolved inorganic carbon and dissolved organic carbon of the European Continental Rivers for the years 1977–2002. *Berichte aus dem Zentrum für Meeres- und Klimaforschung der Universität Hamburg, Reihe B: Ozeanographie*, vol. 48, 159pp.
- Peterson, B.J., 1980. Aquatic primary productivity and the $14\text{C}-\text{CO}_2$ method. A history of the productivity problem. *Annual Review of Ecology and Systematics* 11, 359–365.
- Pohlmann, T., 1996. Predicting the thermocline in a circulation model of the North Sea—part I: model description, calibration and verification. *Continental Shelf Research* 16 (2), 131–146.
- Pohlmann, T., 2006. A meso-scale model of the central and southern North Sea: consequences of an improved resolution. *Continental Shelf Research* 26, 2367–2385.
- Reid, P.C., Lancelot, C., Gieskes, W.W.C., Hagmeier, E., Weichart, G., 1990. Phytoplankton of the North Sea and its dynamics: a review. *Netherlands Journal of Sea Research* 26 (2–4), 295–331.
- Schartau, M., Engel, A., Schröter, J., Thoms, S., Völker, C., Wolf-Gladrow, D., 2007. Modelling carbon overconsumption and the formation of extracellular particulate organic carbon. *Biogeosciences* 4, 433–454.
- Schiettecatte, L.-S., Thomas, H., Bozec, Y., Borges, A.V., 2007. High temporal coverage of carbon dioxide measurements in the Southern Bight of the North Sea. *Marine Chemistry* 106 (1–2), 161–173.
- Smith, S.L., Yamanaka, Y., Kishi, M.J., 2005. Attempting consistent simulations of str. ALOHA with a multi-element ecosystem model. *Journal of Oceanography* 61, 1–23.
- Takahashi, T., et al., 2009. Climatological mean and decadal change in surface ocean pCO₂, and net sea–air CO₂ flux over the global oceans. *Deep-Sea Research II* 56, 554–577, doi:10.1016/j.dsr2.2008.12.009.
- Thomas, H., 2002. Shipboard report of the R/V *Pelagia* cruises 64PE184, 64PE187, 64PE190 and 64PE195. Technical Report 63, Royal Netherlands Institute for Sea Research, Texel, NL.
- Thomas, H., Bozec, Y., Elkalay, K., de Baar, H.J.W., 2004. Enhanced open ocean storage of CO₂ from shelf sea pumping. *Science* 304, 1005–1008.
- Thomas, H., Bozec, Y., Elkalay, K., de Baar, H.J.W., Borges, A.V., Schiettecatte, L.S., 2005. Controls of the surface water partial pressure of the CO₂ in the North Sea. *Biogeosciences* 2, 323–334.
- Thomas, H., Schiettecatte, L.-S., Suykens, K., Koné, Y.J.M., Shadwick, E.H., Prowe, A.E.F., Bozec, Y., de Baar, H.J.W., Borges, A.V., 2009. Enhanced ocean carbon storage from anaerobic alkalinity generation in coastal sediments. *Biogeosciences* 6, 267–274.
- Toggweiler, J.R., 1993. Carbon overconsumption. *Nature* 363, 210–211.
- Tsunogai, S., Watanabe, S., Sato, T., 1999. Is there a “continental shelf pump” for the absorption of atmospheric CO₂?. *Tellus* 51B, 701–712.
- Williams, P.J., 1990. The importance of losses during microbial growth: commentary on the physiology, measurement and ecology of the release of dissolved organic material. *Marine Microbial Food Webs* 4, 175–206.
- Zhou, J., Mopper, K., Passow, U., 1998. The role of surface-active carbohydrates in the formation of transparent exopolymer particles by bubble adsorption of sea waters. *Limnology and Oceanography* 43 (8), 1860–1871.